$(3 + 1)$-spectrum of neutrino masses: A chance for LSND?

O. L. G. Peres[1,2] * and A. Yu. Smirnov[1,3]

(1) The Abdus Salam International Centre for Theoretical Physics, I-34100 Trieste, Italy

(2) Instituto de Física Gleb Wataghin, Universidade Estadual de Campinas, UNICAMP

13083-970 Campinas SP, Brazil

(3) Institute for Nuclear Research of Russian Academy of Sciences, Moscow 117312,

Russia

Abstract

If active to active neutrino transitions are dominant modes of the atmospheric $(\nu_\mu \to \nu_\tau)$ and the solar neutrino oscillations $(\nu_e \to \nu_\mu/\nu_\tau)$, as is indicated by recent data, the favoured scheme which accommodates the LSND result – the so called (2+2)-scheme – should be discarded. We introduce the parameters η_s^{atm} and η_s^{sun} which quantify an involvement of the sterile component in the solar and atmospheric neutrino oscillations. The (2+2)-scheme predicts $\eta_s^{atm} + \eta_s^{sun} = 1$ and the experimental proof of deviation from this equality will discriminate the scheme. In this connection the (3+1)-scheme is revisited in which the fourth (predominantly sterile) neutrino is isolated from a block of three flavour neutrinos by the mass gap $\Delta m_{LSND}^2 \sim (0.4 - 10)$ eV^2. We find that in the $(3 + 1)$-scheme the LSND result can be reconciled with existing bounds on ν_e- and ν_μ - disappearance at $95 - 99\%$ C.L.. The generic prediction of the scheme is the ν_e- and ν_μ - disappearance probabilities at the level of present experimental bounds. The possibility to strengthen the bound on ν_μ- disappearance in the KEK – front detector experiment is studied. We consider phenomenology of the $(3 + 1)$-scheme, in particular, its implications for the atmospheric neutrinos, neutrinoless double beta decay searches, supernova neutrinos and primordial nucleosynthesis.

---

*Permanent address: Instituto de Física Gleb Wataghin, UNICAMP, Campinas, Brazil.

1 Introduction

It is widely accepted that simultaneous explanation of the solar [1, 2], atmospheric [2–4] and LSND results [5–7] in terms of neutrino conversion requires an existence of the sterile state [8,9]. Less appreciated and discussed fact is that explanation of the LSND result in the favored 4ν-schemes implies that the solar or atmospheric neutrinos (or both) are converted to sterile state. Indeed, it is claimed [8,9] that the only 4ν-schemes which can explain the LSND result and accommodate oscillation solutions of the solar and atmospheric neutrino problems are the schemes of the $(2 + 2)$ type. According to the $(2 + 2)$ - scheme, four neutrino mass eigenstates form two nearly degenerate pairs separated by the gap $\Delta m^2 = \Delta m^2_{LSND} \sim 1$ eV^2. Splittings between masses within pairs are much smaller: they are determined by $\Delta m^2_{atm} \approx 3 \cdot 10^{-3}$ eV^2 in the atmospheric neutrino pair and $\Delta m^2_\odot \lesssim 10^{-4}$ eV^2 in the solar neutrino pair.

The key feature of the $(2 + 2)$-scheme which allows one to get a large enough probability of the $\bar{\nu}_\mu \rightarrow \bar{\nu}_e$ transition and to satisfy existing bounds on mixing parameters is that ν_e and ν_μ are present in different pairs: ν_e is mainly distributed in the pair with $\Delta m^2_\odot$ - splitting, whereas ν_μ is mainly distributed in the pair with Δm^2_{atm} - splitting. Indeed, the depth of the $\bar{\nu}_\mu \leftrightarrow \bar{\nu}_e$ oscillations driven by Δm^2_{LSND} equals

$$\sin^2 2\theta_{LSND} = 4 \, (\sum_{j=3,4} U_{\mu j} U_{ej})^2 = 4 \, (\sum_{j=1,2} U_{\mu j} U_{ej})^2 \sim \epsilon^2, \tag{1}$$

where summation is over the mass eigenstates in the heavy (or light) degenerate pair. If we introduce small parameter ϵ which describes admixture of ν_e (or ν_μ) in the pair where it is not a dominant component, then taking into account that in a given pair either $U_{\mu j} \approx O(1)$ or $U_{ej} \approx O(1)$, we get that the effective mixing is of the order ϵ^2.

The sterile neutrino can be distributed in two pairs in different ways, and there are two extreme versions of the $(2 + 2)$-scheme. 1) The sterile neutrino is mainly in the solar pair, so that the $\nu_e \rightarrow \nu_s$ conversion is responsible for the solution of the solar neutrino problem, whereas atmospheric neutrino problem is solved by $\nu_\mu \leftrightarrow \nu_\tau$ oscillations. 2) The sterile

neutrino is in the atmospheric pair, then ν_μ oscillates into ν_s and the solar neutrino problem is solved by the $\nu_e \leftrightarrow \nu_\tau$ conversion. The intermediate situations are possible when both the solar and atmospheric neutrinos partly oscillate to the sterile component. The exceptional case is when ν_s is distributed equally in the solar and atmospheric neutrino pairs. In all other cases the sterile neutrino contributes either to solar or to atmospheric neutrinos more than one half.

In the alternative $(3+1)$-scheme (see Fig. 1), three mass eigenstates form "flavour block" which has predominantly active flavour with small admixture of the sterile state and small mass splitting. The fourth mass eigenstate is separated from the flavour block by the LSND mass gap $\Delta m^2_{LSND} \approx (0.4 - 10)$ eV^2; it consists mainly of the sterile neutrino with small admixtures of active neutrinos: $|U_{s4}|^2 \approx 1$, $|U_{\alpha4}|^2 << 1$, $\alpha = e, \mu$ and τ. (In general, there is mixing of ν_s and ν_τ in ν_4 and in the flavor block [10].) In the $(3+1)$-scheme the atmospheric and solar neutrino data are explained by the $\nu_\mu \rightarrow \nu_\tau$ oscillations and $\nu_e \rightarrow \nu_\mu/\nu_\tau$ conversion respectively.

It is claimed that the $(3+1)$-mass scheme can not reproduce large enough probability of the $\bar{\nu}_\mu \rightarrow \bar{\nu}_e$ oscillations to explain the LSND result [8,9]. Indeed, the depth of $\bar{\nu}_\mu \rightarrow \bar{\nu}_e$ oscillations driven by the Δm^2_{LSND} equals

$$\sin^2 2\theta_{LSND} = 4\,U^2_{\mu4}U^2_{e4} \sim \epsilon^4, \tag{2}$$

where $U_{\mu4}$ and U_{e4}, are the admixtures of the ν_e and ν_μ in the 4th mass eigenstate. These admixtures are small $(\sim \epsilon)$ being restricted by the accelerator and reactor experiments. As a consequence, the depth of oscillations is of the fourth order in the small parameter. Notice, however, that early analysis of data (with small statistics) showed that the bounds from accelerator and reactors experiments and the positive LSND result can be reconciled in the context of one level dominance scheme at 99% C.L. [11].

There are three recent results which may change eventually the situation in favor of the $(3+1)$-scheme:

1. The data on atmospheric neutrinos (specifically on zenith angle distribution of the upward-going muons, on the partially contained multi-ring events, with $E_\nu > 5$ GeV, and on the enriched neutral current event sample) disfavour oscillations to the sterile state [12]. The $\nu_\mu \leftrightarrow \nu_s$ oscillations can be accepted by the data at 3σ level. Oscillations of active neutrinos, $\nu_\mu \to \nu_\tau$, give better fit of the experimental results.

2. Conversion of solar ν_e neutrinos to active neutrinos gives better global fit of experimental results than conversion to sterile neutrinos [2].

   If active neutrino channels dominate both in the solar and in atmospheric neutrino oscillations, the $(2 + 2)$ -mass scheme should be discarded and the oscillation interpretation of the LSND result becomes problematic. In this connection, we have reconsidered the possibility to explain LSND results in the $(3 + 1)$ -mass scheme [13].

3. Latest analysis of the LSND data [7] shows in further shift of the allowed region of oscillation parameters to smaller values of mixing angle. This leads to a better agreement between the bounds obtained in CDHS [14], CCFR [15] and Bugey [16] experiments and the LSND result in the context of $(3 + 1)$-mass scheme [10, 17, 18].

In this paper we elaborate on the phenomenology of the $(3 + 1)$-scheme which can accommodate the oscillation interpretation of the LSND result. In sect. 2 we introduce parameters η_s^{sun} and η_s^{atm} which quantify participation of the sterile neutrino in the solar and atmospheric neutrino oscillations. We show how these parameters can be used to disentangle the $(2 + 2)$- and $(3 + 1)$-schemes. In sect. 3 we analyze the $\bar\nu_\mu \to \bar\nu_e$ oscillation probability in the $(3+1)$-scheme. We estimate the confidence level for the bound on $\sin^2 2\theta_{e\mu}$ from ν_μ-and ν_e-disappearance experiments. In sect. 4, we study a possibility to improve the bounds on ν_μ-disappearance, and consequently, on $\sin^2 2\theta_{e\mu}$ with the KEK - front detectors experiments. In sect. 5, we describe phenomenological implications of the $(3+1)$-scheme for atmospheric neutrinos, neutrinoless double beta decay searches, primordial nucleosynthesis and supernova neutrinos. In sect. 6 we summarize our results and discuss perspectives to

identify $(3+1)$-mass scheme. In Appendix, we evaluate how strongly the LSND oscillation probability can be enhanced in the schemes with more than one sterile neutrino.

2 The $(2+2)$-scheme versus $(3+1)$-scheme

As we have pointed out in the introduction, the present data disfavor pure $\nu_\mu \leftrightarrow \nu_s$ oscillations of the atmospheric neutrinos and moreover pure $\nu_e \to \nu_s$ conversion is not the best solution of the solar neutrino problem. Let us consider a general case when ν_s is involved both in the solar and in the atmospheric neutrino oscillations.

2.1 Excluding the $(2+2)$-scheme ?

For definiteness we will consider the $(2+2)$-scheme with ν_1 and ν_2 being the "solar" pair of the eigenstates with $\Delta m_\odot^2 \equiv m_2^2 - m_1^2$ mass splitting and ν_3 and ν_4 – the atmospheric pairs (with $\Delta m_{atm}^2 \equiv m_4^2 - m_3^2$ mass splitting ($m_1 < m_2 < m_3 < m_4$). To a good approximation (as far as solar and atmospheric neutrinos are concerned) we can neglect small admixtures of ν_e and ν_μ implied by the LSND result. So, the ν_e-flavor is present in the solar pair:

$$|U_{e1}|^2 + |U_{e2}|^2 \approx 1 \ , \tag{3}$$

and the ν_μ flavor is in the atmospheric pair:

$$|U_{\mu3}|^2 + |U_{\mu4}|^2 \approx 1 \ . \tag{4}$$

Under conditions (3) and (4) the effect of the sterile neutrino both in solar and in atmospheric neutrinos is described by a unique parameter [19]. In what follows, we will introduce this parameter in a more transparent way. Notice that since both solar and atmospheric neutrino oscillations are reduced to 2ν cases, there is no CP-violation effect and the absolute values of mixings are relevant only.

In general, ν_τ and ν_s are mixed both in the solar and atmospheric neutrino pairs. Using the unitarity of the mixing matrix and the equality (3) it is easy to show that in the solar pair (ν_1, ν_2) the electron neutrino mixes with the combination:

$$\tilde{\nu} = \cos\alpha\ \nu_s + \sin\alpha\ \nu_\tau, \tag{5}$$

(where α is the arbitrary mixing angle) so that

$$\nu_1 = \cos\theta_\odot\ \nu_e - \sin\theta_\odot\ \tilde{\nu}, \quad \nu_2 = \cos\theta_\odot\ \tilde{\nu} + \sin\theta_\odot\ \nu_e\ . \tag{6}$$

Here $\theta_\odot$ is the angle which appears in the 2ν-analysis of the solar neutrino data. Then as follows from the unitarity and the condition (4), the combination of ν_s and ν_τ orthogonal to that in Eq. (5):

$$\nu' = \cos\alpha\ \nu_\tau - \sin\alpha\ \nu_s, \tag{7}$$

mixes with ν_μ in the atmospheric neutrino pair (ν_3, ν_4):

$$\nu_3 = \cos\theta_{atm}\nu_\mu - \sin\theta_{atm}\nu', \quad \nu_4 = \cos\theta_{atm}\nu' + \sin\theta_{atm}\nu_\mu, \tag{8}$$

where $\theta_{atm} \sim 45^0$ is the mixing angle responsible for oscillations of the atmospheric neutrinos.

Using Eqs. (5, 6) we find

$$\eta_s^{sun} \equiv |U_{s1}|^2 + |U_{s2}|^2 = \cos^2\alpha\ , \tag{9}$$

that is, $\cos^2\alpha$ or η_s^{sun} give the total presence of the sterile neutrino in the solar pair and describe the effects of the sterile component in the solar neutrinos. Similarly, from the Eq. (7, 8) we get

$$\eta_s^{atm} \equiv |U_{s3}|^2 + |U_{s4}|^2 = \sin^2\alpha\ , \tag{10}$$

so, $\sin^2\alpha$ or η_s^{atm} give a total presence of the sterile component in the atmospheric pair.

Clearly, in the $(2 + 2)$-scheme:

$$\eta_s \equiv \eta_s^{sun} + \eta_s^{atm} = 1. \tag{11}$$

5

The schemes with pure $\nu_e \to \nu_s$ conversion of the solar neutrinos and $\nu_\mu \leftrightarrow \nu_\tau$ oscillations of the atmospheric neutrinos correspond to $\cos^2 \alpha = 1$. The opposite situation: the solar $\nu_e - \nu_\tau$ and the atmospheric $\nu_\mu - \nu_s$ transitions corresponds to $\cos^2 \alpha = 0$.

Notice that in notations of Ref. [19] $\cos^2 \alpha \equiv c_{23}^2 \cdot c_{24}^2$.

The equality (11) is a generic property of the $(2 + 2)$-scheme and it can be checked experimentally. One should measure or restrict η_s^{sun} from the solar neutrino data, and independently, η_s^{atm} from the atmospheric neutrino data. According to Eqs. (9) and (5), $\sqrt{\eta_s^{sun}}$ is the admixture of the ν_s in the state

$$\tilde{\nu} = \sqrt{\eta_s^{sun}} \, \nu_s + \sqrt{1 - \eta_s^{sun}} \, \nu_\tau \tag{12}$$

to which the solar ν_e convert. Thus, η_s^{sun} should be determined from the fit of the solar neutrino data in terms of the 2ν mixing of ν_e and $\tilde{\nu}$. Similarly (see Eqs. (7), (10)), $\sqrt{\eta_s^{atm}}$ is the admixture of the ν_s in the state

$$\nu' = \sqrt{\eta_s^{atm}} \, \nu_\tau - \sqrt{1 - \eta_s^{atm}} \, \nu_s \tag{13}$$

to which the atmospheric neutrinos oscillate. Thus, η_s^{atm} can be determined from the 2ν-analysis of the atmospheric neutrino data in terms of $\nu_\mu - \nu'$ mixing.

If it will be proven that

$$\eta_s^{sun} + \eta_s^{atm} < 1 \tag{14}$$

(or larger than 1), the $(2 + 2)$-scheme should be discarded. Let us summarize the present situation. The global analysis of the solar neutrino data [33] shows that for large mixing angle solutions (LMA):

$$\eta_s^{sun} < 0.44 \quad (90\% \text{ C.L.}) , \qquad \eta_s^{sun} < 0.72 \quad (99\% \text{ C.L.}) ; \tag{15}$$

for LOW solution:

$$\eta_s^{sun} < 0.30 \quad (90\% \text{ C.L.}) , \qquad \eta_s^{sun} < 0.77 \quad (99\% \text{ C.L.}) ; \tag{16}$$

and for small mixing angle solution (SMA):

$$\eta_s^{sun} < 0.90 \quad (90\%\text{C.L.}) , \tag{17}$$

and no bound appears at the 99%C.L.. The bound from the SK results on atmospheric neutrino data is [35]:

$$\eta_s^{atm} < 0.67 \quad (90\%\text{C.L.}) . \tag{18}$$

One can get similar bound from the fit of the zenith angle distribution of events detected by MACRO [36]: $\eta_s^{atm} < 0.7$ at 90 % C.L..

Thus, taking the LMA solution, we get

$$\eta_s \equiv \eta_s^{sun} + \eta_s^{atm} < 1.11 \quad (90\%\text{C.L.}), \tag{19}$$

and for the SMA solution: $\eta_s < 1.57$ and for the LOW solution: $\eta_s < 0.97$. That is, at the moment the $(2 + 2)$-scheme is well acceptable. However the forthcoming solar and atmospheric neutrino experiments can significantly strengthen this bound.

Let us consider dependences of various observable on η_s^{sun} and η_s^{atm}.

The solar neutrinos undergo $\nu_e \to \tilde{\nu}$ conversion. Difference of the ν_e and $\tilde{\nu}$ potentials in matter equals

$$V = \sqrt{2}G_F \left(n_e - \eta_s^{sun}\frac{n_n}{2} \right) , \tag{20}$$

where G_F is the Fermi coupling constant, n_e and n_n are the concentrations of electrons and neutrons correspondingly. With the increase of η_s^{sun} the potential decreases, this leads to a shift of the adiabatic edge of the suppression pit to smaller $\Delta m^2/E_\nu$ and to modification (weakening) of the Earth matter effect [39].

One expects an intermediate situation between pure active and pure sterile cases.

Presence of the sterile component in the solar neutrino flux modifies also interactions of neutrinos in detectors. The reduced rate of the neutral current events [NC] defined as the ratio of events with and without oscillations, $N_{NC}(osc)/N_{NC}(SSM)$, decreases with

increase of η_s^{sun}:

$$[\text{NC}] = \eta_s^{sun} \bar{P} + (1 - \eta_s^{sun}), \tag{21}$$

here $\bar{P}$ is the effective (averaged) survival probability. Two remarks are in order.

1). The probability $\bar{P} = \bar{P}(\eta_s^{sun})$ should be calculated with the effective potential (20), although its dependence on η_s^{sun} is rather weak.

2). The probability should be calculated for each specific variable separately (taking into account cross sections, energy thresholds etc.) so that $\bar{P}$ in Eq. (21) may differ from $\bar{P}$ which will appear in the following formulas.

The double ratio - the ratio of the reduced rates of the neutral current events [NC] and the charged current events ([CC] $\equiv N_{CC}(osc)/N_{CC}(SSM)$) changes as:

$$\frac{[\text{NC}]}{[\text{CC}]} = \eta_s^{sun} + \frac{1 - \eta_s^{sun}}{\bar{P}} . \tag{22}$$

With increase of η_s^{sun} the double ratio decreases from $1/\bar{P}$ to 1. The rate [NC] and the ratio [NC]/[CC] will be measured in the SNO experiment [37].

The reduced charged current event rate [CC] ($\equiv N_{CC}(osc)/N_{CC}(SSM)$) can be written in terms of the suppression factor for the $\nu - e$ event rate, $R_{\nu e} \equiv N_{\nu e}(osc)/N_{\nu e}(SSM)$, as

$$[\text{CC}] = \frac{R_{\nu e}}{1 - r(1 - \eta_s^{sun})(1 - 1/\bar{P})} . \tag{23}$$

Here $r \equiv \sigma(\nu_\mu e)/\sigma(\nu_e e)$ is the ratio of the cross-sections of the muon and the electron neutrino scattering on the electron. The rate $R_{\nu e}$ is measured with high precision at Super-Kamiokande and it will be also measured at SNO. According to (23), with increase of involvement of the sterile neutrino the rate increases from $R_{\nu e}/(1 - r(1 - 1/\bar{P}))$ for the pure active case to $R_{\nu e}$ for the pure sterile neutrino case.

The presence of the sterile component in the atmospheric neutrinos can be established by studies of the neutral current interaction rates. The suppression factor for the π^0-event rate in the pure sterile case is expected to be about $\xi = 0.7 - 0.8$ [38]. In general case the

8

ratio of π^0 to e-like event rates is suppressed as

$$\frac{N(\pi^0)}{N_e} = \frac{N^0(\pi^0)}{N_e^0}(1 - \eta_s^{atm} + \xi\eta_s^{atm}) \,, \tag{24}$$

where $N^0(\pi^0)$ and N_e^0 are the numbers of events with and without oscillations.

Appearance of the ν_τ in oscillations of ν_μ is suppressed by the factor $\cos^2 \alpha \equiv 1 - \eta_s^{atm}$. This can be tested in the long base-line experiments. One can compare the mixing parameter $\sin^2 2\theta_{\mu\mu}$ extracted from studies of the ν_μ - disappearance and the parameter $\sin^2 2\theta_{\mu\tau}$ found from the ν_τ - appearance experiments. In the $(2+2)$-scheme one expects

$$\frac{\sin^2 2\theta_{\mu\tau}}{\sin^2 2\theta_{\mu\mu}} = 1 - \eta_s^{atm}. \tag{25}$$

Also the zenith angle distribution of the of multi-ring events from the so called NC enriched sample [12] is sensitive to η_s^{atm}.

The Earth matter effect on atmospheric ν_μ neutrino oscillations depends on η_s^{atm}. The matter potential for $\nu_\mu - \nu'$ system equals:

$$V = \sqrt{2}G_F\frac{n_n}{2}\eta_s^{atm}. \tag{26}$$

The potential increases with η_s^{atm}, and one expects an intermediate situation between active and sterile neutrino cases [34, 35]. For high energy upward going muons the suppression of the oscillation effect increases with η_s^{atm}. The effect is more complicated for neutrinos crossing the core of the earth where the parametric enhancement of oscillations may take place.

2.2   The $(3+1)$-scheme and mixing of sterile neutrino

In the $(3+1)$-scheme with 4th (isolated) mass eigenstate being predominantly sterile one, total involvement of the sterile neutrino in the solar and atmospheric neutrino oscillations

can be very small. If the ν_τ component in the ν_4 is absent, we have from unitarity condition

$$\sum_{i=1}^{3} U_{si}^2 = |U_{e4}|^2 + |U_{\mu 4}|^2 < (3 - 10) \cdot 10^{-2} \tag{27}$$

where the inequality corresponds to the CDHS and Bugey bounds.

The situation is different if ν_τ mixes with ν_s in the 4th eigenstate [10]. Now ν_4 consists mainly of the combination

$$\tilde{\nu} = \cos \beta \; \nu_s + \sin \beta \; \nu_\tau \tag{28}$$

with small admixtures of ν_e and ν_μ implied by the LSND experiment ($\nu_4 \approx \tilde{\nu}$). The mixing in the flavor block can be obtained from the one in the original $(3 + 1)$-scheme (without $\nu_s - \nu_\tau$ mixing) by substituting $\nu_\tau \to \nu'$, where

$$\nu' = \cos \beta \; \nu_\tau - \sin \beta \; \nu_s. \tag{29}$$

is the orthogonal combination to that in Eq. (28).

An immediate consequence of the $\nu_\tau - \nu_s$ mixing is an appearance of $\nu_\tau \leftrightarrow \nu_s$ oscillations driven by Δm_{LSND}^2 [10]. The depth of these oscillations equals $\sin^2 2\beta$.

Due to the presence of ν_μ in ν_4 described by $U_{\mu 4}$ the scheme leads also to $\nu_\mu \leftrightarrow \nu_\tau$ oscillations with $\Delta m^2 = \Delta m_{LSND}^2$ and the depth

$$\sin^2 2\theta_{\mu\tau} \simeq 4|U_{\mu 4}|^2 \sin^2 \beta = \sin^2 2\theta_{\mu\mu} \cdot \sin^2 \beta \; , \tag{30}$$

where $\sin^2 2\theta_{\mu\mu}$ describes the disappearance of ν_μ. Eq. (30) allows to get the upper bound on $\sin^2 \beta$. Indeed, using $\sin^2 2\theta_{\mu\tau}(C/N)$ – the upper bound on $\sin^2 2\theta_{\mu\tau}$ from the CHORUS [40] and NOMAD [41] experiments and taking $\sin^2 2\theta_{\mu\mu}$ at the upper edge allowed by the CDHS experiment (as is implied by the LSND result) we get:

$$\sin^2 \beta \leq \frac{\sin^2 2\theta_{\mu\tau}(C/N)}{\sin^2 2\theta_{\mu\mu}(CDHS)} \; . \tag{31}$$

From this formula we find that for $\Delta m^2 < 2$ eV^2 no bound appears; for $\Delta m^2 = 4, 6, 8$ eV^2 we get $\sin^2 \beta < 0.32, 0.13, 0.06$ correspondingly.

10

In the presence of $\nu_\tau - \nu_s$ mixing the solar ν_e will convert into the combination

$$\nu_\mu \cos\theta_{atm} + \nu_\tau \sin\theta_{atm} \cos\beta - \nu_s \sin\theta_{atm} \sin\beta. \tag{32}$$

If SMA is the solution for solar neutrino problem then the above state is roughly $(\approx \nu_2)$.

That is, the contribution of the sterile component is determined by the product $\sin\theta_{atm} \cdot \sin\beta$ and therefore

$$\eta_s^{sun} = \sin^2\theta_{atm} \sin^2\beta \tag{33}$$

(instead of $\cos^2\alpha$ in the $(2+2)$-scheme).

Due to $\nu_\tau - \nu_s$ mixing the atmospheric ν_μ will oscillate with $\Delta m^2 = \Delta m_{atm}^2$ into the state ν' (see Eq. (29)). According to (29), the admixture of the sterile component is $\sin\beta$, so that

$$\eta_s^{atm} = \sin^2\beta. \tag{34}$$

From (33) and (34) we find that the total effect of the sterile components in the solar and atmospheric neutrino oscillations can be described by

$$\eta_s = \eta_s^{sun} + \eta_s^{atm} = \sin^2\beta \cdot (1 + \sin^2\theta_{atm}). \tag{35}$$

The parameter η_s can be larger than 1 since in the $(3+1)$-scheme we make the double counting of the ν_s contributions from the two lightest states (they contribute both to η_s^{sun} and to η_s^{atm}). In contrast with the $(2+2)$-scheme, now η_s is not fixed and it can change from $(1 + \sin^2\theta_{atm})$ to practically zero when $\sin^2\beta \to 0$.

According to Eqs. (34) and (33)

$$\eta_s^{sun} = \sin^2\theta_{atm}\eta_s^{atm}, \tag{36}$$

so that the inequality $\eta_s^{sun} \le \eta_s^{atm}$ is the generic property of the $(3+1)$-scheme under consideration. Taking $\sin^2\theta_{atm} < 0.67$ (which corresponds to the lower bound $\sin^2 2\theta_{atm} > 0.88$ from the Super-Kamiokande data) we get from (33) and (18): $\eta_s^{sun} < 0.45$ independently

on solution of the solar neutrino problem. This bound is stronger than the immediate bound from the solar neutrino data.

3   LSND oscillation probability in the $(3+1)$-scheme

Let us consider predictions for the $\bar{\nu}_\mu \rightarrow \bar{\nu}_e$ oscillations relevant for the LSND result. The short range oscillation results are determined by one Δm^2_{LSND} only (flavour block is "frozen") and the oscillation pattern is reduced to the 2ν neutrino oscillations. So, one can use immediately the results of the analysis of the LSND data in terms of the 2ν-oscillations. The depth of the oscillations or the effective mixing parameter is given in Eq. (2). As in the one level dominance scheme [32], it is determined by the admixtures of ν_e and ν_μ in the isolated state. This prediction does not depend on mixing in the flavour block, in particular, on the solution of the solar neutrino problem.

Mixing matrix elements which enter the expression for $\sin^2 2\theta_{e\mu}$ (2) are restricted by short baseline experiments. In the range of Δm^2 relevant for the LSND result the best bound on U^2_{e4} is given by the Bugey reactor experiment [16]. The ν_e-survival probability in this experiment is determined by

$$\sin^2 2\theta_{ee} = 4\,U^2_{e4}(1 - U^2_{e4}) \approx 4\,U^2_{e4}. \tag{37}$$

The best bound on $U^2_{\mu4}$, for 0.3 eV^2 < Δm^2 < 8 eV^2, follows from the ν_μ-disappearance searches in the CDHS experiment [14]. The relevant mixing parameter equals

$$\sin^2 2\theta_{\mu\mu} = 4\,U^2_{\mu4}(1 - U^2_{\mu4}) \approx 4\,U^2_{\mu4}. \tag{38}$$

From Eqs. (2), (37) and (38) we get unique relation between the depths of oscillations in the CDHS, Bugey and LSND experiments:

$$\sin^2 2\theta_{e\mu} \approx \frac{1}{4}\sin^2 2\theta_{ee} \cdot \sin^2 2\theta_{\mu\mu}. \tag{39}$$

This relation holds in the one level dominance scheme when only one Δm^2 contributes to oscillations in all three experiments. The relation is modified in more complicated situations, e.g., in schemes with more than one sterile neutrino.

The Bugey [16] and CDHS [14] experiments have published the 90% C.L. upper bounds on $\sin^2 2\theta_{ee}$ and $\sin^2 2\theta_{\mu\mu}$ as functions of the Δm^2. These bounds transfer immediately to the bounds on $U_{\mu4}^2$ and U_{e4}^2:

$$U_{e4}^2 \lesssim U_{Bugey}^2(\Delta m^2), \tag{40}$$

$$U_{\mu4}^2 \lesssim U_{CDHS}^2(\Delta m^2).$$

Using Eq. (37) and Eq. (38) one gets the upper bound on $\sin^2 2\theta_{e\mu}$ [8,9]:

$$\sin^2 2\theta_{e\mu} = 4\, U_{\mu4}^2 U_{e4}^2 \lesssim 4\, U_{Bugey}^2(\Delta m^2) \cdot U_{CDHS}^2(\Delta m^2). \tag{41}$$

The bound (41) shown in Fig. 2 excludes most of the region of parameters indicated by the LSND experiment. On this basis, it was concluded that $(3+1)$ -mass scheme cannot reproduce the LSND result [8,9]. The question is, however, which confidence level should be ascribed to the bound (41)? Or, at which confidence level the LSND result is excluded by the combined Bugey and CDHS bounds?

Let us introduce the probabilities, $P_\alpha(U_{\alpha4}^2, \Delta m^2)$, $\alpha = e, \mu$, that experimental data from Bugey or CDHS correspond to a given value of $U_{\alpha4}^2$ for fixed Δm^2. The probabilities $P_\alpha(U_{\alpha4}^2, \Delta m^2)$ should be found from the fit of experimental data. In such a fit $U_{\alpha4}^2$ can take both positive and negative values but with $|U_{\alpha4}^2| < 1$. Therefore the normalization conditions for P_α should be written as $\int_{-\infty}^{\infty} dx P_\alpha(x, \Delta m^2) = 1$. The 90% C.L. bounds on $U_{\alpha4}^2$ are determined by the condition

$$\int_{-\infty}^{U_{\alpha4}^2} dx P_\alpha(x, \Delta m^2) = 0.9 \;. \tag{42}$$

The probability that the product of $U_{e4}^2 \cdot U_{\mu4}^2$ is larger than certain value ρ is given by the integral

$$\mathcal{P}(\rho) \equiv \int_{\rho}^{\infty} dy \int_{\rho/y}^{\infty} dx P_e(x, \Delta m^2) P_\mu(y, \Delta m^2). \tag{43}$$

13

The 95% and 99% C.L. upper bounds, ρ_{95} and ρ_{99}, are determined by the conditions

$$\mathcal{P}(\rho = \rho_{95}) = 0.05, \qquad \mathcal{P}(\rho = \rho_{99}) = 0.01 . \tag{44}$$

It is impossible to reconstruct the probabilities, $P_\alpha(U_{\alpha 4}^2, \Delta m^2)$, from published 90% C.L. exclusion plots. Therefore to make estimations, we adopt the following procedure:

1). We assume that the distributions $P_\alpha(U_{\alpha 4}^2, \Delta m^2)$ have the Gaussian form. The latter is characterized by central value, $\bar{U}_{\alpha 4}^2$, and by the widths σ_α.

2). For several Δm^2 the experimental groups have published the best fit values of $U_{\alpha 4}^2$ and we use them as the central values $\bar{U}_{\alpha 4}^2$ in the Gaussian distributions.

3). For those Δm^2 we find the widths of the distributions using Eqs. (42) and the published 90% C.L. upper bounds on $U_{\alpha 4}^2 = 1/4 \sin^2 2\theta_{\alpha\alpha}$.

4). Using definitions (44) and Eq. (43), we calculate the 95% C.L. and 99% C.L. bounds, on the products of the matrix elements, and consequently, on $\nu_e - \nu_\mu$ mixing parameter: $\sin^2 2\theta_{e\mu} \leq 4\rho$.

The bounds on $\sin^2 2\theta_{e\mu}$ are shown in Fig. 2 for different values of Δm^2 by rombs and triangles. Also shown, is the 90% C.L. allowed region of LSND taken from Ref. [6]. As follows from the figure, in the interval $\Delta m^2 = 0.4 - 2$ eV^2, some part of the LSND region is compatible with the Bugey and CDHS bounds at $95 - 99\%$ C.L. . The upper limit given by the product of the bounds corresponds to 95% C.L. in the range of $\Delta m^2 \lesssim 1$ eV^2 and it approaches 99% C.L. for smaller values of Δm^2.

For $\Delta m^2 < 0.7$ eV^2, the bound from CDHS disappears and stronger restriction on $\sin^2 2\theta_{\mu\mu}$ follows from the atmospheric neutrino results, namely, from the up-down asymmetry which becomes suppressed when large admixture of ν_μ exists in the heavy state [8].

Thus, the LSND result is consistent with bounds on mixing from other experiments at a few per cent level in the of the $(3 + 1)$-scheme.

Introduction of more than 1 sterile neutrino can enhance the LSND probability. The

enhancement consistent with bounds on the ν_e - and ν_μ - disappearance is however rather weak: about 20 % (see Appendix).

4   Improving the bounds on ν_μ- and ν_e- disappearance

Explanation of the LSND result in the (3+1)-scheme implies that both U_{e4}^2 and $U_{\mu 4}^2$ are close to their present upper experimental bounds. If ν_4 consists mainly of the sterile component, the dominant modes of oscillations will be $\nu_e \leftrightarrow \nu_s$ and $\nu_\mu \leftrightarrow \nu_s$. If ν_4 contains significant admixture of the ν_τ, one should expect also $\nu_\mu \leftrightarrow \nu_\tau$ and $\nu_e \leftrightarrow \nu_\tau$ oscillations [10]. Therefore, further (even moderate) improvements of sensitivities of the oscillation searches with respect to the Bugey and CDHS sensitivities should lead to discovery of oscillations both in ν_e- and in ν_μ- disappearance. Negative results of these searches will exclude the oscillation interpretation of the LSND result in the $(3 + 1)$-scheme.

Let us consider possibilities to improve bounds on ν_μ- and ν_e- oscillation disappearance searches in the forthcoming experiments.

4.1 ν_e- disappearance experiments

The $\bar{\nu}_e$- disappearance due to oscillations with $\Delta m^2 = \Delta m_{LSND}^2 = (0.4 - 10)$ eV^2 can be searched for in the high statistics short base-line reactor experiments of the Bugey type. Keeping in mind restricted power of the reactors the only possibility to significantly increase statistics is to increase the size of the detector placed close to the reactor. Notice that the absolute value of the neutrino flux is known with an accuracy about 3 - 5 %, and therefore to improve substantially the Bugey bound one should search for the non-averaged oscillation effects. Notice that for $\Delta m^2 \sim 1$ eV^2 and $E = 3$ MeV the oscillation length equals $l_\nu \sim 7-8$ m which is on the border of the averaging regime.

No experiments of this type are planned now, and it seems, the Bugey bounds on U_{e4}^2

will not be improved before Mini-BooNE will report its results [20].

The reactor project can be considered if Mini-BooNE will confirm the LSND result. Such an experiment will allow to disentangle the $(2 + 2)$ and $(3+1)$-schemes. Indeed, in the $(2 + 2)$-scheme one expects small ν_e-disappearance effect which can be described by the mixing parameter of the order the LSND mixing parameter: $\sin^2 2\theta_{ee} = 4(U_{e3}^2 + U_{e4}^2) \sim 2 \sin^2 2\theta_{LSND}$. That is, the positive effect of oscillations in the short-baseline reactor experiment will exclude the $(2 + 2)$-scheme.

4.2 ν_μ - disappearance and KEK - front detector experiment

Let us consider a possibility to improve bound on $U_{\mu 4}^2$ using KEK front detectors [21]. At KEK the high intensity ν_μ-flux with energies 0.5 - 3 GeV (maximum at 1 GeV) is formed in the decay pipe of the length 200 m. Two front detectors are situated at the distance about 100 m from the end of the pipe. At the Fine Grained Detector (FGD) one expects to observe about 9200 μ - like events for 1. 10^{-20} protons on target (P.O.T.) , whereas at the 1 kton water Cherenkov detector the number of events is 30 times larger.

One can search for the ν_μ-disappearance by measuring the energy distribution of the μ - like events. Let us evaluate the sensitivity of such a study. We calculate the ratios of numbers of events in the energy bins i: $E_\mu^i \div E_\mu^i + \Delta E_\mu$ with (N_{osc}^i) and without (N_0^i) oscillations:

$$R_i \equiv \frac{N_{osc}^i}{N_0^i} \ . \tag{45}$$

The ratios can be written in the following way:

$$R_i \approx \frac{1}{N} \int_{E_\mu^i}^{E_\mu^i + \Delta E} dE_\mu \int_0^\infty dE_\mu' f(E_\mu, E_\mu') \int_{E_\mu'}^\infty dE_\nu F(E_\nu) \sigma(E_\nu, E_\mu') \bar{P}(E_\nu) \ , \tag{46}$$

where $f(E_\mu, E_\mu')$ is the (muon) energy resolution function, $F(E_\nu)$ is the neutrino flux at the front detector [23], $\sigma(E_\nu, E_\mu^i)$ is the total inclusive cross section of the $\nu_\mu N \to \mu X$ reaction [22]. It is dominated by quasi-elastic cross-section with sub-leading contributions

16

from other reactions in the energy range of the KEK experiment ($E_\mu^{max} \lesssim 3$ GeV). In our calculations we use the quasi-elastic cross section only. N is the normalization factor which equals the integral (46) with $\bar{P} = 1$. In Eq. (46), $\bar{P}(E_\nu)$ is the neutrino survival probability averaged over the production region:

$$\bar{P}(E_\nu) = \frac{1}{N_P(E_\nu)} \int_0^{x_p} dx (L-x)^{-2} P(E_\nu, L-x) e^{-\frac{\gamma(E_\nu)x}{\tau_\pi}} . \tag{47}$$

Here

$$\gamma(E_\nu) = \frac{E_\nu}{k m_\pi}$$

is the effective Lorentz factor of pions which produce neutrinos with the energy E_ν and $k = 0.488$, m_π and τ_π are the mass and the lifetime of the pion; $L \approx 300$ m is the distance between the beginning of the decay pipe and the front detectors, x_p is the length of the pipe. In Eq. (47) N_P is the normalization factor which equals the same integral with $P = 1$.

Since the energy resolution is rather good and the size of the energy bin is smaller than typical energy scale of the probability changes we omit the integration over E_μ and E_μ' and in the rest of integration take $E_\mu' = E_\mu^i$.

The results of calculations of R_i are shown in the Fig. 4 for several values of Δm^2 and mixing angles at the border of the region excluded by the CDHS experiment. The characteristic oscillation pattern is clearly seen for large $\Delta m^2 \gtrsim 6$ eV^2. For $\Delta m^2 \lesssim 1$ eV^2, we find very smooth distortion of spectrum with increasing deficit at events of low energies. The deficit is at most 10%. As follows from the figure, with further increase of statistics the KEK front detector may improve the CDHS bounds on $U_{\mu 4}^2$ in the high Δm^2 part of the LSND allowed region.

It would be interesting to estimate the possibility of water Cherenkov front detector [23] where the statistics should be about 30 times higher than in FGD. The problem here is that the muons with $E_\mu > 1.6$ GeV [24] are not contained inside the detector [26] and therefore the higher part of muon spectrum cannot be measured.

Let us underline that in this section we have described results of simplified estimations

and the detailed study of possibilities by the experimental groups are necessary.

4.3   Mini-BooNE experiment, and the neutrino mass spectrum

In the case of positive result of the $\nu_\mu - \nu_e$ oscillation searches by the Mini-BooNE we will have strong evidence of existence of the sterile neutrino. Moreover, the Mini-BooNE experiment itself may allow us to disentangle the $(3 + 1)$- and $(2 + 2)$-schemes. Indeed, Mini-BooNE can search for the ν_μ - disappearance in the range $\Delta m^2 = (8 \cdot 10^{-2} \div 20)$ eV^2. For $\Delta m^2 \sim 0.6$ eV^2, the sensitivity to the effective mixing parameter can reach 0.15.

In the $(2 + 2)$-scheme the ν_μ-disappearance driven by Δm^2_{LSND} has very small probability suppressed by small admixtures of ν_μ in the "wrong" pair. If ν_μ is mainly in the pair (ν_3, ν_4) then

$$\sin^2 2\theta_{\mu\mu} = 4(U_{\mu1}^2 + U_{\mu2}^2) \ . \tag{48}$$

It is at the level of mixing implied by the LSND: $\sin^2 2\theta_{\mu\mu} < \sin^2 2\theta_{LSND}$.

In contrast, in $(3+1)$-scheme ν_μ-disappearance should be at the level of the bound from the CDHS experiment [14], as is given in Eq. (38). That is, $\sin^2 2\theta_{\mu\mu} \sim \sin^2 2\theta_{\mu e}/U_{e4}^2$ – the mixing parameter is enhanced by the factor $1/U_{e4}^2$.

If the Mini-BooNE experiment will find $\nu_\mu \to \nu_e$ oscillation effect compatible with LSND, but no ν_μ-disappearance will be detected, the $(3+1)$-scheme will be excluded, provided that $\Delta m^2_{LSND} = (2 - 4) \cdot 10^{-1}$ eV^2.

For $\Delta m^2_{LSND} > 4 \cdot 10^{-1}$ eV^2, the sensitivity of Mini-BooNE to ν_μ disappearance is worse than the present bound from CDHS experiment. Much better sensitivity to ν_μ disappearance can be reached in the BooNE experiment. In Fig. 2 we show the restrictions on the LSND oscillation mode from the bounds which can be achieved by the Mini-BooNE and BooNE experiments instead of the CDHS bound.

5 Phenomenology of $(3 + 1)$ -mass scheme

In the "minimal" version of the $(3+1)$-scheme with normal mass hierarchy and small $\nu_s - \nu_\tau$ mixing (one would expect $U_{\tau 4} \sim U_{\mu 4}$), the presence of the sterile neutrino in the flavor block is rather small:

$$\sum_{i=1,2,3} |U_{si}|^2 \sim U_{e4}^2 + U_{\mu 4}^2 \sim (3-10) \cdot 10^{-2} . \tag{49}$$

It will be difficult to detect such admixtures in oscillations driven by $\Delta m_\odot^2$ and Δm_{atm}^2, that is, in the solar, atmospheric and the long base-line experiments. Therefore, new elements of phenomenology of the scheme are associated mainly with the mixing of active neutrinos in the 4th (isolated) mass eigenstate.

5.1 Neutrinoless Double beta decay

If neutrinos are the Majorana particles, the double beta decay, $\beta\beta_{0\nu}$, can put bounds on the mixing parameters. Indeed, the $(3 + 1)$-scheme predicts the value for the effective Majorana mass of the electron neutrino, m_{ee}, which can be accessible for the future $\beta\beta_{0\nu}$ measurements. If the spectrum has normal mass hierarchy with the isolated state being the heaviest one, the dominant contribution follows from this heaviest state:

$$m_{ee} \sim m_{ee}^{(4)} \equiv U_{e4}^2 \sqrt{\Delta m_{LSND}^2}. \tag{50}$$

The upper limit on m_{ee} as a function of Δm_{LSND}^2 in the allowed region of the LSND result is shown in Fig. 3. The Heidelberg-Moscow present limits on m_{ee} is showed [27]. As follows from the figure the next generation of $\beta\beta 0\nu$ experiments, the GENIUS (1 ton version) [28], the EXO and CUORE [29] will be able to test this scenario. For preferable values $\Delta m^2 \sim (1-2)$ eV^2 we get from (50) $m_{ee} \sim (1-2) \cdot 10^{-2}$ eV.

The $(3 + 1)$-scheme with inverted mass hierarchy in which the three active states form degenerate triplet with $m > (0.4 - 10)$ eV is restricted already by present data. The bound on $\beta\beta_{0\nu}$ rate [27] implies large mixing angle solutions of the solar neutrino problem (LMA,

LOW, VO) and cancellations of contributions to m_{ee} from different mass eigenstates [30].

5.2 Atmospheric neutrinos

The survival probability for the atmospheric muon neutrinos equals:

$$P_{\mu\mu} \equiv 1 - 2U_{\mu4}^2 - 4U_{\mu3}^2(1 - U_{\mu3}^2 - U_{\mu4}^2)\sin^2\Delta m_{atm}^2, \tag{51}$$

where we have averaged over oscillations driven by the mass split, Δm_{LSND}^2. According to Eq. (51), the shape of the zenith angle distribution and the up-down asymmetry are determined by the effective mixing parameter

$$\sin^2(2\theta_{atm}^{eff}) = \frac{4\,U_{\mu3}^2(1 - U_{\mu3}^2 - U_{\mu4}^2)}{1 - 2U_{\mu4}^2} \approx 4\,U_{\mu3}^2(1 - U_{\mu3}^2 + U_{\mu4}^2). \tag{52}$$

Notice that this parameter can be bigger than 1: e.g., for $U_{\mu3}^2 = 1/2$ and $U_{\mu4}^2 = 2{\cdot}10^{-2}$ we get $\sin^2 2\theta_{atm}^{eff} \approx 1.04$. This can explain an appearance of unphysical values of $\sin^2 2\theta_{atm}^{eff}$ in the fits of the zenith angle distributions. For small values of Δm_{LSND}^2, where the CDHS bound is weaker or absent, $U_{\mu4}$ can be large enough and an enhancement of $\sin^2 \theta_{atm}^{eff}$ can be significant. The presence of additional sterile state suppresses the average survival probability

$$\langle P_{\mu\mu}\rangle \equiv 1 - 2(U_{\mu4})^2 - 2U_{\mu3}^2(1 - U_{\mu3}^2 - U_{\mu4}^2). \tag{53}$$

5.3 Nucleosynthesis bound

Sterile neutrinos are generated in the Early Universe due to oscillations $\nu_e \leftrightarrow \nu_s$ and $\nu_\mu \leftrightarrow \nu_s$ driven by Δm_{LSND}^2 and mixing of ν_e and ν_μ in the isolated 4th state. The mixing parameters for $\nu_e \to \nu_s$ and $\nu_\mu \to \nu_s$ channels, $\sin^2 2\theta_{es} \sim 4U_{e4}^2$ and $\sin^2 2\theta_{\mu s} \sim 4U_{\mu4}^2$, are big enough, so that oscillations will lead to the equilibrium concentration of ν_s. Thus in the epoch of primordial nucleosynthesis ($T \sim$ few MeV) one expects the presence of four neutrino species

in equilibrium. The current limit, $N_\nu < 3.4$, can be avoided if large enough lepton asymmetry ($\sim 10^{-5}$) existed already before oscillations driven by the Δm^2_{LSND} became efficient ($T \sim 10$ MeV). In this case, the asymmetry suppresses oscillations in the $\nu_e \rightarrow \nu_s$ and $\nu_\mu \rightarrow \nu_s$ channels. Notice however, that large lepton asymmetry cannot be produced in the scheme itself by the oscillations to sterile neutrinos and anti-neutrinos: the mechanism [42] does not works. It requires the active neutrino state to be heavier than sterile state and very small mixing of sterile neutrinos in that heavier state. Another way to avoid the bound is to assume that active neutrinos were not in equilibrium before nucleosynthesis epoch [43]. In this case, the number of additional neutrino species can be even larger than 1.

5.4 Supernova neutrinos

Physics of the supernova neutrinos can be significantly modified by presence of the sterile component.

The difference of the matter potentials for ν_e and ν_s in electrically neutral medium equals

$$V_{es} = \sqrt{2} G_F n_e \left[1 - \frac{n_n}{2n_e} \right] + V_\nu = \frac{G_F n}{\sqrt{2}} (3Y_e - 1) + V_\nu , \tag{54}$$

where n is the total nucleon density; $Y_e \equiv n_e/n$ is the number of electrons per nucleon; V_ν is the potential due to neutrino-neutrino scattering which is important in the region close to the neutrinosphere.

Typical dependence of the potential V_{es} on distance [45, 46] is shown in Fig. 5 . For the neutrino channel the potential is negative in the central parts; it becomes zero when $Y_e \approx 1/3$, then it changes the sign, reaches maximum and then falls down with density. The potential changes also with time: the gradients become larger. Moreover, after several seconds another region with strong neutronization ($Y_e < 1/3$) may appear at densities below 10^7 g/cc. An appearance of this region is related to the conversion $\nu_e \rightarrow \nu_s$ in the outer resonance (see later). As a consequence, the reaction $\bar{\nu}_e + p \rightarrow e^+ + n$ will dominate over

$\nu_e + n \to e^- + p$, thus producing the neutron reach region. It was suggested [47] that in this region the nucleosynthesis of heavy elements may take place.

For the $\nu_\mu - \nu_s$ channel the difference of potentials equals

$$V_{\mu s} = \frac{G_F n}{\sqrt{2}}(1 - Y_e) + V_\nu'. \tag{55}$$

Crossings of the ν_e- and ν_s- levels are determined by the condition:

$$\frac{\Delta m_{LSND}^2 \cos 2\theta}{2E} - V_{es} = 0 \ . \tag{56}$$

For the anti-neutrino channels V_{es} or the first term should be taken with opposite sign. Similar equation should be written for the potential $V_{\mu s}$.

In Fig. 5 the points of the resonances are shown as crossings of the V_{es} with the horizontal lines given by $\approx \Delta m^2/2E$ (lines below $V = 0$ correspond to the anti-neutrino channel).

From (54) and (56) we find the resonance densities (for $V_\nu = 0$):

$$n = \frac{\Delta m_{LSND}^2 \cos 2\theta}{2E} \frac{\sqrt{2}}{G_F(3Y_e - 1)} \ . \tag{57}$$

Using the potentials (54),(20) and resonance conditions (56) we can construct the level crossing scheme. The scheme for the $(3 + 1)$ spectrum with normal mass hierarchy is shown in fig. 6. We use the flavor basis $(\nu_s, \nu_e, \nu_\mu^*, \nu_\tau^*)$, where ν_μ^*, ν_τ^* are the states which diagonalize the ν_μ - ν_τ sub-matrix of the total mass matrix. This rotation allows us to remove large mixing and it does not change the physics since the produced ν_μ and ν_τ fluxes are practically identical and they can not be distinguished at the detection.

The adiabaticity condition in the $\nu_e - \nu_s$ resonances can be written as $\gamma \gg 1$, where the adiabaticity parameter equals

$$\gamma = 4\pi^2 \frac{l_0 \cdot l_Y}{3l_\nu^2} \sin^2 2\theta \left[Y_e + \frac{l_Y}{l_n} \left(Y_e - \frac{1}{3} \right) \right]^{-1} \ . \tag{58}$$

Here $l_Y \equiv Y_e/(dY_e/dx)$, $l_n \equiv n/(dn/dx)$, $l_\nu = 4\pi E/\Delta m^2$, $l_0 = \sqrt{2}m_N/G_F\rho$ are the vacuum oscillation length and the refraction length.

22

In the case of normal mass hierarchy in the neutrino channels there are two crossings of the ν_s and ν_e levels determined by the condition (56) (see Fig. 5). One (outer) crossing occurs at relatively low density $\rho_r \sim 10^6 g/cm^3 (\Delta m^2_{LSND}/1eV^2)$ [48], when Y_e substantially deviates from $1/3$ ($Y_e \sim 0.5$) (see Fig. 6). It is characterized by the mixing parameter $\sin^2 2\theta_{es} \sim 4U^2_{e4}$ ($4U^2_{e4} \cos\beta^2$ in general). This resonance is highly adiabatic: the resonance density is relatively small, so that the refraction length is large. Also the gradients of the density and electron number are rather small. For $E \leq 40$ MeV, and $\sin^2 2\theta = 4 \cdot 10^{-2}$ we find that $\gamma \geq O(10)$ in the relevant range $\Delta m^2_{LSND} = (0.4 \div 10)$ eV^2.

Thus, in the outer resonance the ν_e converts almost completely to ν_s with survival probability

$$P_{ee} \approx U^2_{e4} < (2-3) \cdot 10^{-2} \; . \tag{59}$$

If $\Delta m^2_{LSND} > 2$ eV^2, the ν_e-flux is absent above the layers with $\rho \sim (10^6 - 10^7)$g/cc, that is, in the region where r-processes can lead to synthesis of heavy elements [47]. An absence of the ν_e-flux enhances an efficiency of the r-processes. For $\Delta m^2_{LSND} \lesssim 1$ eV^2 the effect of conversion on the r-processes is weak.

The second (inner) crossing occurs at much higher densities $\rho \sim 10^{11}$ g/cm^3 [44] in the layers with significant neutronization when

$$Y_e \approx 1/3$$

(see Fig. 5). Here the neutrino-neutrino scattering gives substantial contribution to V_{es} which shifts the resonance. The level crossing occurs mainly due to change of the chemical composition (the ratio $n_n/n_e = n_n/n_p$). Taking $n \cdot m_N = 10^{10}$ g/cc, (m_N is the nucleon mass), $l_Y = 3$ km, $E = 10$ MeV, $\Delta m^2 = 10$ eV^2 and $\sin^2 2\theta_{es} = 0.1$ we get for the adiabaticity parameter $\gamma \sim 0.3$, that is, the adiabaticity is broken. For $\Delta m^2 > 30$ eV^2 the adiabaticity could be satisfied. This leads to disappearance of the $\bar{\nu}_e$-flux. Therefore observation of the anti-neutrino signal from SN1987A excludes such a possibility thus putting the upper bound on Δm^2. (Notice that the ν_e-flux regenerates in the outer resonance

23

destroying conditions for the r-processes). At later time, gradients of density and Y_e become larger, in particular, $l_Y \sim 0.3$ km, so that the adiabaticity breaks down even for large Δm^2.

For $\Delta m^2 < 2$ eV^2 the adiabaticity is strongly broken for neutrinos of the detectable energies, $E > 5$ MeV, during all the time of the burst and the effect of the inner resonance can be neglected.

Let us consider properties of the neutrino bursts arriving at the Earth detectors.

1). The generic prediction of the scheme is disappearance of the "neutronization peak" due to $\nu_e \rightarrow \nu_s$ conversion in the outer resonance (59) . The peak should be seen neither in ν_e nor in ν_μ/ν_τ. Observation of the peak in the ν_e luminosity at the initial stage will exclude the scheme with normal mass hierarchy. Only if the inner resonance is adiabatic the scheme can survive.

2). During the cooling stage one expects hard ν_e-spectrum which coincides with original spectrum of ν_μ and/or ν_τ: $F(\nu_e) \propto F^0(\nu_\mu)$. The absolute value of the ν_e-flux depends on the mixing in the flavour block. If $U_{e3}^2 > 10^{-3}$, so that the level crossing related to Δm^2_{atm} is adiabatic, one gets $F(\nu_e) = F^0(\nu_\mu)$ independently on solution of the solar neutrino problem. No Earth matter effect should be observed. If $U_{e3}^2 < 10^{-5}$, the level crossing is strongly non-adiabatic and the ν_e-signal depends on properties of the low density resonance related to the $\Delta m^2_\odot$. For the LMA solution one gets: $F(\nu_e) = \cos^2 \theta_\odot F^0(\nu_\mu)$. The flux can be larger in the case of SMA (small mixing angle) solution depending on the level of adiabaticity. Intermediate situation is possible, if U_{e3}^2 is in the interval $10^{-5} - 10^{-3}$.

In the antineutrino channels, the $\bar{\nu}_s$-level does not cross $\bar{\nu}_e$ level but it has two crossings with $\bar{\nu}_\mu^*$ and $\bar{\nu}_\tau^*$ levels which can be both adiabatic. Still the presence of the sterile neutrino will modify the $\bar{\nu}_e$ signal. The $\bar{\nu}_e$ propagation is adiabatic so that $\bar{\nu}_e \rightarrow \bar{\nu}_1$. If SMA solution is correct, one gets $\bar{\nu}_1 \approx \bar{\nu}_e$, that is $\bar{\nu}_e$-flux is practically unchanged. For LMA (or LOW) the soft part of the spectrum will be suppressed:

$$F(\bar{\nu}_e) = \cos^2 \theta_\odot F^0(\bar{\nu}_e) \tag{60}$$

and the total $\bar{\nu}_e$ flux will depend on characteristics of $\bar{\nu}_s - \bar{\nu}_\mu/\nu_\tau$ resonances. At least one of these resonances should be adiabatic since the mixing of $\bar{\nu}_s$ in the active block is $\sum_{i=1}^{3} U_{si}^2 \geq U_{e4}^2 + U_{\mu 4}^2$ and the later is large enough. If $\bar{\nu}_s$ crossing with $\bar{\nu}_\mu^*$ is adiabatic, then $\bar{\nu}_\mu^* \rightarrow \bar{\nu}_s$ and the $\bar{\nu}_e$ flux will be as in Eq. (60). If the resonance is completely non-adiabatic, then $\bar{\nu}_\mu^* \rightarrow \bar{\nu}_2$, and since $\bar{\nu}_2$ has a component $\sin^2 \theta_\odot$ of the $\bar{\nu}_e$-flux we get $F(\bar{\nu}_e) = \cos^2 \theta_\odot F^0(\bar{\nu}_e) + \sin^2 \theta_\odot F^0(\bar{\nu}_\mu)$. In these cases also the Earth matter effect should be observed.

Some combination of the $\bar{\nu}_\mu$ and $\bar{\nu}_\tau$ fluxes, will be converted to the sterile neutrino flux.

In the case of inverted mass hierarchy, when the isolated fourth state is the lightest one, the crossings of $\bar{\nu}_e$ and $\bar{\nu}_s$ levels appear in the antineutrino plane. As the result, originally produced $\bar{\nu}_e$ will be converted to $\bar{\nu}_s$. For $\Delta m_{LSND}^2 > 2$ eV^2 this will dump the efficiency of the r-processes.

The $\bar{\nu}_e$ flux at the Earth will be formed in the conversion of $\bar{\nu}_\mu$ and $\bar{\nu}_\tau$ to $\bar{\nu}_e$ due to the mixing in the flavor block: more precisely, in the resonance associated with $\Delta m_\odot^2$. In the case of SMA solution this conversion is practically absent, so that no $\bar{\nu}_e$-flux is expected at the Earth in contradiction with observations of the $\bar{\nu}_e$-burst from SN1987A. Therefore the SN1987A data require one of the large mixing solutions. In the case of LMA or LOW solutions one expects $F(\bar{\nu}_e) \sim \sin^2 \theta_\odot F^0(\bar{\nu}_\mu)$. Properties of the ν_e-flux are determined by mixing in the flavour block [30].

6 Discussions and conclusions

1. Simultaneous explanation of the LSND result as well as the solar and atmospheric neutrino data in terms of neutrino oscillations requires introduction of additional (sterile) neutrino. In the favored $(2+2)$ - scheme the sterile component should be involved significantly in the conversion of the solar and atmospheric neutrinos.

2. Recent experimental results give an indication that both in solar and in atmospheric

neutrinos the oscillation channels to active component dominate. We show that in the (2 + 2)-scheme the equality $\eta_s^{sun} + \eta_s^{atm} = 1$ should be fulfilled. The statistically significant deviation from this equality, in particular, a proof that $\eta_s = \eta_s^{sun} + \eta_s^{atm} < 1$ will lead to rejection of the (2 + 2)-scheme.

In the case of $(3 + 1)$-scheme η_s^{atm} can take any value between ≈ 0 and $1 + \sin^2 \theta_{atm}$. The generic prediction of the scheme is that $\eta_s^{sun} \leq \eta_s^{atm}$.

Determination of η_s from analysis of the solar and atmospheric neutrino data will allow us to disentangle the (2 + 2) and $(3 + 1)$-schemes.

We show that the LSND result can be reconciled with the bounds on ν_e- (Bugey) and $\nu_\mu-$ (CDHS) disappearance at 95 % - 99% C.L.. The best agreement can be achieved at $\Delta m^2 = (1 - 2)$ eV^2.

4. The key consequences of the $(3 + 1)$-scheme which explains the LSND result are that the probabilities of the $\nu_e \leftrightarrow \nu_s$ and $\nu_\mu \leftrightarrow \nu_s$ oscillations with $\Delta m^2 = \Delta m^2_{LSND}$ should be at the level of present upper bounds, so that moderate improvements of the bounds should lead to discovery of oscillations in these channels. We have estimated the possibility of the KEK - front detectors experiments to improve the bound on ν_μ disappearance. We show that for $\Delta m^2 > 6$ eV^2 searches of the distortion of the energy spectrum of the μ-like events may have better sensitivity to oscillations than CDHS has. The Mini-BooNE experiment can improve the CDHS bound for $\Delta m^2 < 0.6$ eV^2 and the BooNE experiment will have better sensitivity than CDHS for $\Delta m^2 < 1$ eV^2.

At the moment, no experiment is planned to improve the Bugey bound on $\bar{\nu}_e$-disappearance in the range $\Delta m^2 = \Delta m^2_{LSND}$. The relevant experiment could be the one with large size detector situated close to the reactor. Such an experiment will deserve serious consideration if Mini-BooNE confirms the LSND result or/and some indications of the sterile neutrino involvement are seen in the solar and atmospheric neutrino experiments.

5. In the $(3 + 1)$-scheme the effective Majorana mass of the electron neutrino can be

about $2 \cdot 10^{-2}$ eV for the normal mass hierarchy and at the level of the upper experimental bound in the case of inverted mass hierarchy.

6. The scheme can reproduce an "unphysical" value of the effective mixing parameter: $\sin^2 2\theta^{eff} > 1$ in the two neutrino analysis of the atmospheric neutrino data.

7. The scheme predicts that a sterile neutrino was in the thermal equilibrium in the epoch of primordial nucleosynthesis unless "primordial" lepton asymmetry suppressed the oscillations of active to sterile neutrinos.

8. Presence of the sterile neutrino in the $(3 + 1)$-scheme can substantially influence the physics of supernova neutrinos. The $(3 + 1)$-scheme with normal mass hierarchy and $\Delta m^2 > 2$ eV^2 can realize mechanism of disappearance of the ν_e-flux from the region with densities $(10^6 - 10^8)$ g/cc, thus creating necessary conditions for the nucleosynthesis of the heavy elements in the r-processes (see however [46]).

The scheme predicts disappearance of the neutronization peak and hard ν_e- spectrum during the cooling stage. The presence of sterile neutrino can manifest itself also as suppression of the $\bar{\nu}_e$ flux without change of the spectrum.

Let us outline further developments.

1). Before Mini-BooNE result, the progress will be related to further searches for the sterile neutrino components in the solar and atmospheric neutrinos. The experimental groups are requested to get bounds on η_s^{sun} and η_s^{atm} parameters from the one Δm^2 fit of their results.

Important bounds will come from the SNO experiment: namely, from measurements of the CC event rate and comparison of this rate with the neutrino-electron scattering rate, from searches for the Earth regeneration effects and the distortion of the spectrum, from measurements of the NC-event rates and the double ratio $[NC]/[CC]$.

As far as the atmospheric neutrino data are concerned, further accumulation of data on

the zenith angle distributions and neutral current interactions will strengthen the bound on η_s^{atm}. Here the distributions of the upward going muons and the events in the NC - enriched samples, as well as measurements of π^0 events rate are of special interest.

Still it is difficult to expect that the bound $\eta_s < 1$ will be established at the high confidence level.

2). The Mini-BooNE experiment will give the key result which will determine further developments. In the case of negative result, still searches for the sterile neutrinos will be continued with some other motivation. The positive result will give strong confirmation of existence of the sterile neutrino, and identification of correct four (or more) states scheme will be the major issue.

Notice that values of the $\sin^2 2\theta_{e\mu}$ at the upper side of the LSND allowed region will favour the $(2 + 2)$-scheme. Also restrictions on Δm^2 (say excluding of $\Delta m^2 > 1$ eV^2) will have important implications.

Mini-BooNE itself and BooNE will search for also ν_μ-oscillation disappearance. Detection of the disappearance will favor the $(3 + 1)$-scheme.

The ORLAND experiment [49] will have sensitivity for $\nu_\mu \to \nu_e$ oscillations which will cover the LSND region.

3). Later progress will be related to searches for the $\nu_\tau-$ appearance and $\nu_\mu-$ disappearance in the long baseline experiments. OPERA [50] will allow one to improve bound on the sterile neutrinos. MINOS experiment [51] will provide a decisive check of presence of sterile neutrinos by measurements of NC/CC ratio.

Special high statistics reactor experiment to search for the $\bar{\nu}_e$-disappearance can be considered.

Future neutrinoless double beta decays searches can give an additional check of the model being especially sensitive to scheme with inverted mass hierarchy.

Appendix. LSND and additional sterile neutrinos

Let us make several remarks on possibility to get larger predicted LSND effect by introducing additional sterile neutrino ν'_s. In general an introduction of additional neutrino state can enhance the LSND probability and/or influence (relax) bounds from the laboratory and atmospheric neutrino experiments on the relevant mixing parameters U_{e4} and $U_{\mu 4}$.

1). To influence the prediction for LSND oscillation probability, the 5th mass eigenstate (being mainly sterile neutrino) should have non-zero mixing with both ν_e and ν_μ. If ν_5 has admixture of ν_e (or ν_μ) only, it will open new channels for ν_e-(ν_μ-) disappearance, thus enhancing the bound on U^2_{e4} (or $U^2_{\mu 4}$) from Bugey (CDHS) experiment. At the same time, it will be no additional contribution to the LSND probability in comparation with the $(3+1)$-scheme. As the result, one gets stronger bound on possible value of $\sin^2 2\theta_{e\mu}$,

$$\sin^2 2\theta_{e\mu} < 4\, U^2_{Bugey}(\Delta m^2) U^2_{CDHS}(\Delta m^2). \tag{61}$$

2). The sensitivities of the Bugey, LSND and CDHS results to Δm^2 have the following hierarchy: $\Delta m^2_{Bugey} < \Delta m^2_{LSND} < \Delta m^2_{CDHS}$. Then depending on value of m^2_5 one can get different situations:

(i) $m^2_5 < \Delta m^2_{Bugey}$: neither bounds on $U^2_{\alpha 4}$ nor the LSND probability are changed.

(ii) $\Delta m^2_{Bugey} < m^2_5 < \Delta m^2_{LSND}$: No additional contribution to the LSND appears. At the same time, new channel will be open for the ν_e-disappearance which leads to stronger bound on U^2_{e4}. As a consequence, the LSND probability will be suppressed.

(iii) $m^2_5 > \Delta m^2_{LSND}$: for mixing angles relevant for the LSND at this condition both bounds on $U^2_{\alpha 4}$ will be modified and the LSND will get an additional contribution from the second Δm^2.

The mass m_5 should not be very close to m_4. The splitting should be resolved by the LSND experiment, that is: $\Delta m^2_{54} >> 10^{-2}$ eV^2. Following the analysis of Ref. [8], we find that in the degenerate case, $\Delta m^2_{54} \ll 10^{-2}$ eV^2, the depths of the ν_μ- and ν_e-oscillations

equal

$$\sin^2 2\theta_{\mu\mu} = 4\,\eta_\mu(1-\eta_\mu), \tag{62}$$

$$\sin^2 2\theta_{ee} = 4\,\eta_e(1-\eta_e), \tag{63}$$

where $\eta_\alpha \equiv \sum_{i=4,5} U_{\mu i}^2$, $\alpha = e, \mu$. The depth of the $\nu_\mu \to \nu_e$ channel driven by Δm_{LSND}^2 is

$$\sin^2 2\theta_{LSND} = 4\sum_{i=4,5} U_{\mu i}^2 U_{ei}^2 \leq 4\sum_{i=4,5} U_{\mu i}^2 \sum_{i=4,5} U_{ei}^2 = \eta_e \eta_\mu = \frac{1}{4}\sin^2 2\theta_{ee} \times \sin^2 2\theta_{\mu\mu}\,, \tag{64}$$

where we have used the Schwartz inequality. Comparing result in (64) with the one in (39) we see that the LSND probability in the scheme with additional neutrino is smaller than in the $(3+1)$-scheme.

As an example, we have considered the neutrino mass spectrum with (i) $\Delta m_{4i}^2 \approx (1-2)$ eV^2, where index $i = 1,2,3$ enumerates the eigenstates from the flavour block, (ii) $\Delta m_{5i}^2 \geq 8$ eV^2 and (iii) non-zero admixtures, U_{e5} and $U_{\mu 5}$, of the ν_e and ν_μ in the 5th state. So, both necessary conditions discussed above are satisfied. Oscillations associated with the 5th state are averaged in the Bugey and LSND experiments and they are at least partly averaged in the CDHS experiment.

In the mass range, $\Delta m_{5i}^2 > 8$ eV^2, the CDHS bound is rather weak and stronger bound on the $U_{\mu 5}^2$ follows from the CCFR experiment [15]. This CCFR bound on $U_{\mu 5}^2$ is still a factor of two weaker than the CDHS bound on $U_{\mu 4}^2$ at $\Delta m^2 = (1-2)$ eV^2. Taking also $U_{e5}^2 \sim U_{e4}^2 \sim U_{Bugey}^2/2$ we have found that the probability of $\bar{\nu}_\mu \leftrightarrow \bar{\nu}_e$ oscillations can be enhanced by a factor 1.25 at most with respect to result of the $(3+1)$-scheme (see Eq. (2)).

Notice also that introduction of the second sterile neutrino can further aggravate a situation with primordial nucleosynthesis.

Acknowledgments

Note added

After this work was accomplished the paper [52] has appeared in which the possibility to constraint the η_s^{atm} parameter to be down to 0.3 using the energy distribution of the CC and NC events at MINOS was discussed.

References

[1] SAGE Collaboration, V. Gavrin *et. al*, talk at Neutrino 2000 conference, 15-21 June 2000, Sudbury, Canada. ; GNO Collaboration, E. Bellotti, *et. al*, talk at Neutrino 2000 conference, 15-21 June 2000, Sudbury, Canada.; Homestake Collaboration, K. Lande *et. al*, talk at Neutrino 2000 conference, 15-21 June 2000, Sudbury, Canada. Transparencies available at http://nu2000.sno.laurentian.ca.

[2] Super-Kamiokande Collaboration, Y. Suzuki *et. al*, talk at Neutrino 2000 conference, 15-21 June 2000, Sudbury, Canada. Transparencies available at http://nu2000.sno.laurentian.ca.

[3] Soudan Collaboration, T. Mann *et. al*, talk at Neutrino 2000 conference, 15-21 June 2000, Sudbury, Canada. Transparencies available at http://nu2000.sno.laurentian.ca.

[4] MACRO Collaboration, B. Barish *et. al*, talk at Neutrino 2000 conference, 15-21 June 2000, Sudbury, Canada. Transparencies available at http://nu2000.sno.laurentian.ca.

[5] C. Athanassoupoulos *et. al*, Phys. Rev. Lett. **75** (1995) 2650; Phys. Rev. **C54** (1996) 2685; Phys. Rev. Lett. **77** (1996) 3082; Phys. Rev. Lett. **81** (1998) 1774; Phys. Rev. **C 58** (1998) 2489.

[6] K. Eitel, New Jour. Phys. **2** (2000) 1. Available at http://www.njp.org/ ; hep-ex/9909036.

[7] LSND Collaboration, G. Mills *et. al* talk at Neutrino 2000 conference, 15-21 June 2000, Sudbury, Canada. Transparencies available at http://nu2000.sno.laurentian.ca.

[8] S. M. Bilenky, C. Giunti and W. Grimus, Eur. Phys. J. **C1** (1998) 247; S. M. Bilenky, C. Giunti, W. Grimus and T. Schwetz, Phys. Rev. **D60** (1999) 073007.

[9] V. Barger, S. Pakvasa, T. J. Weiler and K. Whisnant, Phys. Rev. **D58** (1998) 093016; V. Barger, T. J. Weiler and K. Whisnant, Phys. Lett. **B427** (1998) 97 .

[10] C. Giunti and M. Laveder, hep-ph/0010009.

[11] G.L. Fogli, E. Lisi, G. Scioscia, Phys. Rev. **D56** (1997) 3081.

[12] Super-Kamiokande Collaboration, T. Kajita *et. al*, talk at NOW 2000 conference, 6-9 September 2000, Otranto, Italy. Transparencies available at http://www.ba.infn.it/ now2000/ ; hep-ex/0009001.

[13] A. Yu. Smirnov, talk at the APS Meeting (Long Beach, April 2000); A. Yu. Smirnov, talk at Neutrino 2000 conference, 15-21 June 2000, Sudbury, Canada. Transparencies available at http://nu2000.sno.laurentian.ca; hep-ph/0010097.

[14] CDHS Collaboration, F. Dydak *et. al*, Phys. Lett. **B134** (1984) 281.

[15] CCFR Collaboration, I. E. Stockdale *et. al*, Z. Phys. **C27** (1985) 53.

[16] Bugey Collaboration, B. Achkar *et. al*, Nucl. Phys. **B434** (1995) 503.

[17] V. Barger *et. al*, Phys. Lett. **B489** (2000) 345.

[18] Boris Kayser, hep-ph/0010206.

[19] C. Giunti, M.C. Gonzalez-Garcia and C. Peña-Garay, Phys. Rev. **D62** (2000) 013005.

[20] Mini-BooNE collaboration, E. Church *et al.*, nucl-ex/9706011; Available at http://www-boone.fnal.gov/BooNE/boone_proposal.ps.

[21] K2K Collaboration, K. Nishikawa *et. al*, KEK-PS Proposal, Nucl. Phys. B (Proc. Suppl.) **59** (1997) 289; K2K Collaboration, K. Nakamura *et. al*, talk at Neutrino 2000 conference, 15-21 June 2000, Sudbury, Canada. Transparencies available at http://nu2000.sno.laurentian.ca.

[22] P. Lipari, M. Lusignoli and F. Sartogo, Phys. Rev. Lett. **74** (1995) 4384.

[23] K2K Collaboration, Y. Oyama *et. al*, Talk at XXXV Rencontres de Moriond "Electroweak interactions and unified theories", Les Arcs, Savoie, France, March 11-18, 2000; hep-ex/0004015; A copy of this talk is available at http://neutrino.kek.jp/ oyama/moriond_transparencies/.

[24] C. Yanagisawa, private communication.

[25] K2K Collaboration, M. Sakuda *et. al*, Talk at XXXth International Conference on High Energy Physics, July 27 - August 2, 2000, Osaka, Japan. Transparencies available at http://www.ichep2000.rl.ac.uk/.

[26] J. Hill, private communication.

[27] Heidelberg-Moscow Collaboration, H.V. Klapdor *. et. al.* , talk at NOW 2000 conference, 6-9 September 2000, Otranto, Italy. Transparencies available at http://www.ba.infn.it/ now2000/.

[28] GENIUS Collaboration, H.V. Klapdor *. et. al.* , talk at NOW 2000 conference, 6-9 September 2000, Otranto, Italy. Transparencies available at http://www.ba.infn.it/ now2000/.

[29] For the EXO/CUORE experiments, B. Bettini, talk at NOW 2000 conference, 6-9 September 2000, Otranto, Italy. Transparencies available at http://www.ba.infn.it/ now2000/.

[30] A. S. Dighe and A. Yu. Smirnov, Phys. Rev. **D62** (2000) 033007.

[31] E776 Collaboration, L. Borodovsky *et. al*, Phys. Rev. Lett. **68** (1992) 274.

[32] A. de Rujula *et al.*, Nucl. Phys. **B168** (1980) 54; V. Barger and K. Whisnant, Phys. Lett. **B209** (1988) 365; S. M. Bilenky *et al.*, Phys. Lett. **B276** (1992) 223; H. Minakata, TMUP-HEL-9503 (unpublished); K.S. Babu, J. Pati and F. Wilczek, Phys. Lett. **B359** (1995) 351;(E) **B364** (1995) 251.

[33] M. C. Gonzalez-Garcia, talk at Neutrino 2000 conference, 15-21 June 2000, Sudbury, Canada. Transparencies available at http://nu2000.sno.laurentian.ca.; hep-ph/0010136.

[34] O. Yasuda, hep-ph/0006319.

[35] A. Marrone, talk at NOW 2000 conference, 6-9 September 2000, Otranto, Italy. Transparencies available at http://www.ba.infn.it/ now2000/; G.L. Fogli, E. Lisi and A. Marrone, hep-ph/0009299.

[36] MACRO Collaboration, F. Ronga *et. al*, talk at NOW 2000 conference, 6-9 September 2000, Otranto, Italy. Transparencies available at http://www.ba.infn.it/ now2000/

[37] A. McDonald, *et. al*, talk at Neutrino 2000 conference, 15-21 June 2000, Sudbury, Canada. Transparencies available at http://nu2000.sno.laurentian.ca.

[38] F. Vissani and A. Yu. Smirnov, Phys. Lett. **B432** (1998) 376.

[39] M. Maris and S. T. Petcov, Phys. Rev. **D58** (1998) 113008.

[40] CHORUS Collaboration, P. Zucchelli *et. al*, talk at NOW 2000 conference, 6-9 September 2000, Otranto, Italy. Transparencies available at http://www.ba.infn.it/ now2000/

[41] NOMAD Collaboration, G. Vidal-Sitjes *et. al*, talk at NOW 2000 conference, 6-9 September 2000, Otranto, Italy. Transparencies available at http://www.ba.infn.it/ now2000/

[42] R. Foot and R.R. Volkas, Phys. Rev. **D56** (1997) 6653; (E) **D59** (1999) 029901; R. Foot, Astropart. Phys. **10** (1999) 253; P. Di Bari and R. Foot, Phys. Rev. **D61** (2000) 105012.

[43] G. Giudice, E. W. Kolb and A. Riotto, hep-ph/0005123.

[44] M.B. Voloshin, Phys. Lett. **B209** (1988) 360.

[45] G. C. McLaughlin, J. M. Fetter, A. B. Balantekin and G. M. Fuller, Phys. Rev. **C59** (1999) 2873.

[46] M. Patel and G. M. Fuller, hep-ph/0003034; Proceedings of the American Physical Society Division of Particles and Fields Conference (DPF'99), UCLA, Jan. 1999, ed. K. Arisaka and Z. Bern.

[47] D. Caldwell, G. M. Fuller and Y.-Z. Qian, Phys. Rev. **D61** (2000)12305 .

[48] A. Yu. Smirnov, Nucl. Phys. Proc. Suppl. **77** (1999) 98; hep-ph/9809481.

[49] Orland Collaboration, F. T. Avignone *et al.*, Phys. At. Nucl. **63** (2000) 1007.

[50] OPERA Collaboration, A. Rubbia *et. al*, talk at Neutrino 2000 conference, 15-21 June 2000, Sudbury, Canada. Transparencies available at http://nu2000.sno.laurentian.ca.

[51] MINOS Collaboration, V. Paolone *et. al*, talk at NOW 2000 conference, 6-9 September 2000, Otranto, Italy. Transparencies available at http://www.ba.infn.it/ now2000/.

[52] MINOS Collaboration, D. A. Petyt, MINOS Note NuMI-L-691, available at http://gate.hep.anl.gov/ndk/hypertext/numi_notes.html (unpublished).
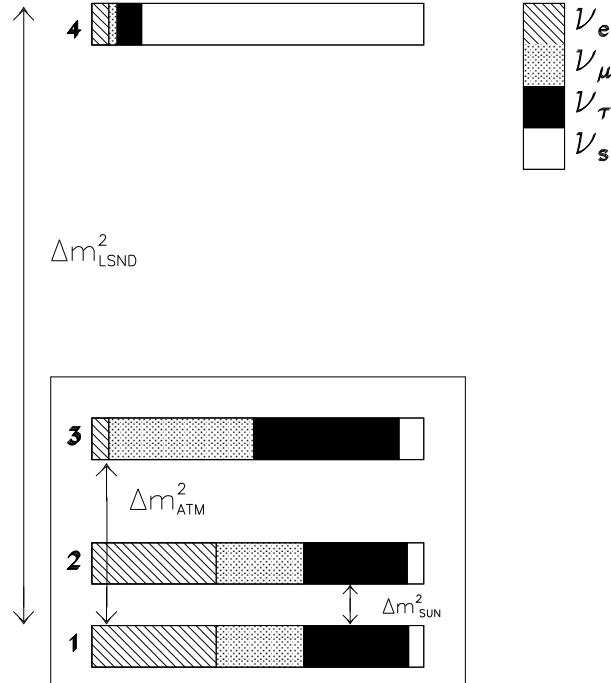
Figure 1: The neutrino mass and flavor spectrum in the $(3+1)$ scheme with normal mass hierarchy. The boxes correspond to the mass eigenstates. The sizes of different regions in the boxes determine flavors of the eigenstates: $|U_{\alpha i}|^2$, $\alpha = e, \mu, \tau, s$, $i = 1, 2, 3, 4$.
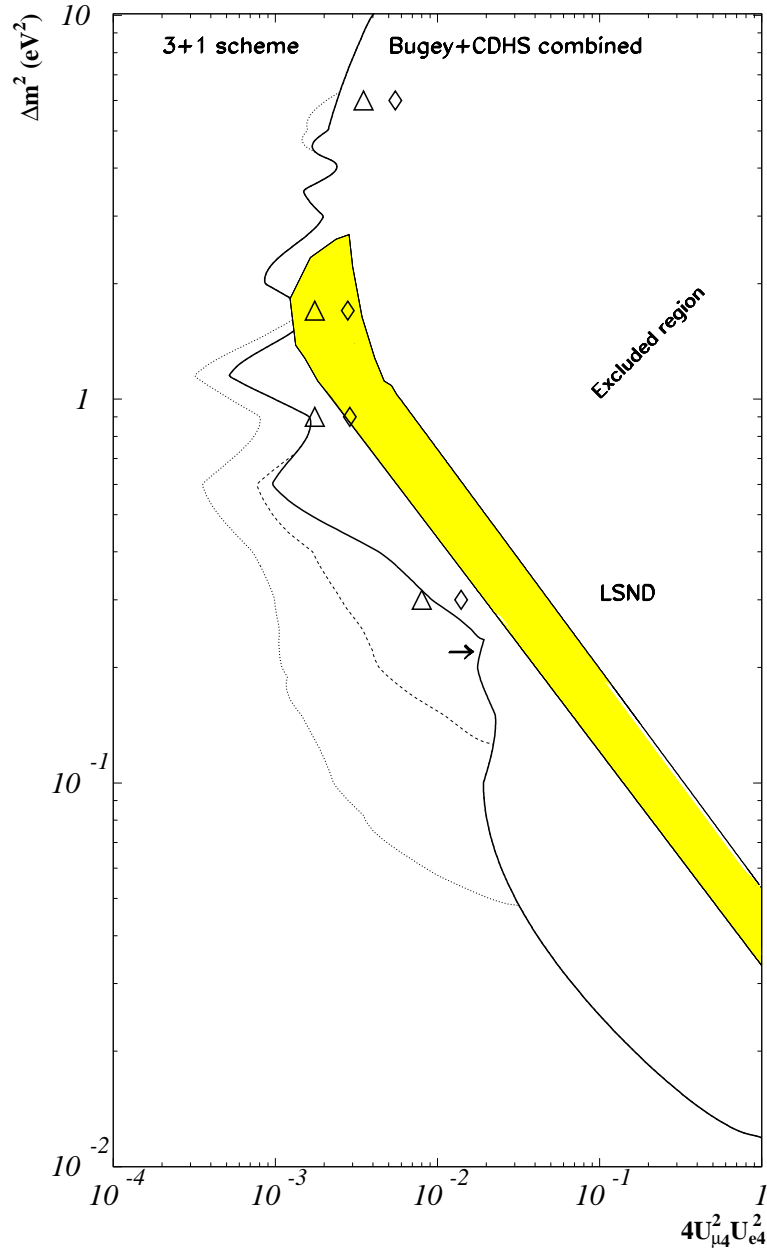
Figure 2:   The LSND allowed region (shadowed) and the bounds on the oscillation parameters in the $(3 + 1)$ - scheme from the ν_e- and $\nu_\mu-$ disappearance experiments. The lines show the limits obtained as the products of the 90 % C.L. upper bounds on $|U_{e4}|^2$ and $|U_{\mu4}|^2$. Solid line is product of the bounds from Bugey and CDHS (above the arrow) and is product of the bounds from Bugey and atmospheric neutrinos (below the arrow). Also shown are the bounds obtained as the product of bound from Bugey and expected bound from Mini-BooNE (dashed line) and BooNE (dotted line) experiments. The triangles and rombs show respectively the 95 and 99 % C.L. bounds obtained in this paper (see Eq. 43).
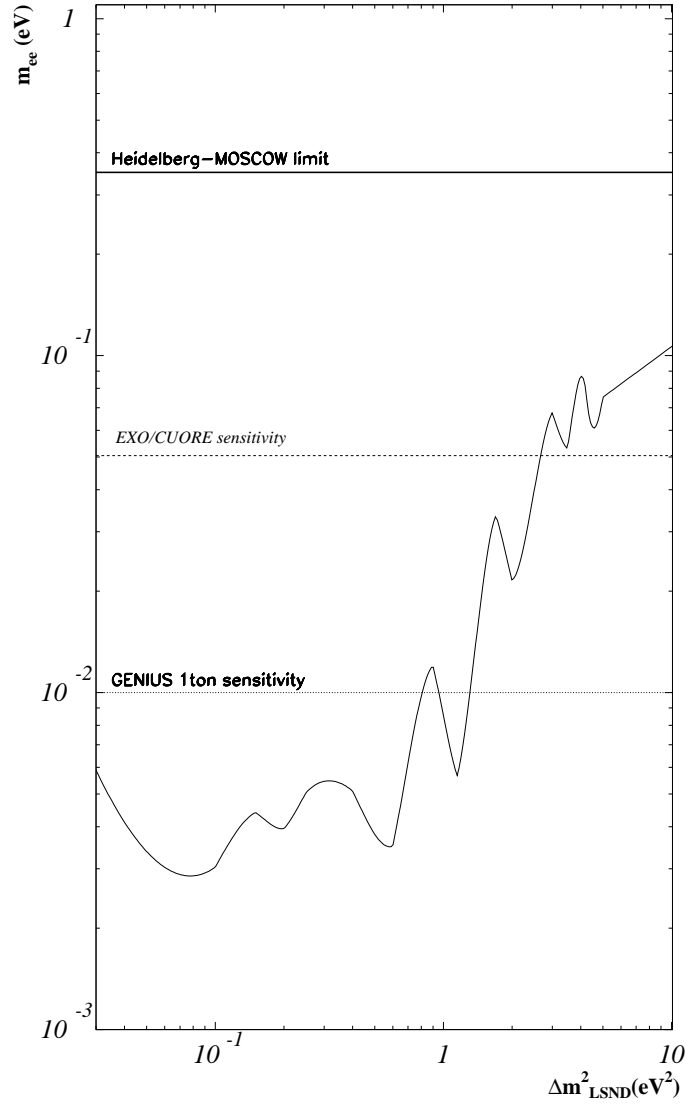
Figure 3: The upper bound on the effective Majorana mass of the electron neutrino m_{ee} as the function of Δm^2_{LSND} in the $(3+1)$ scheme with normal mass hierarchy. The bound corresponds to the upper limit on $|U_{e4}|^2$ from the Bugey experiment. Also shown are the present and future limits on m_{ee} from the $\beta\beta_{0\nu}$ - experiments.
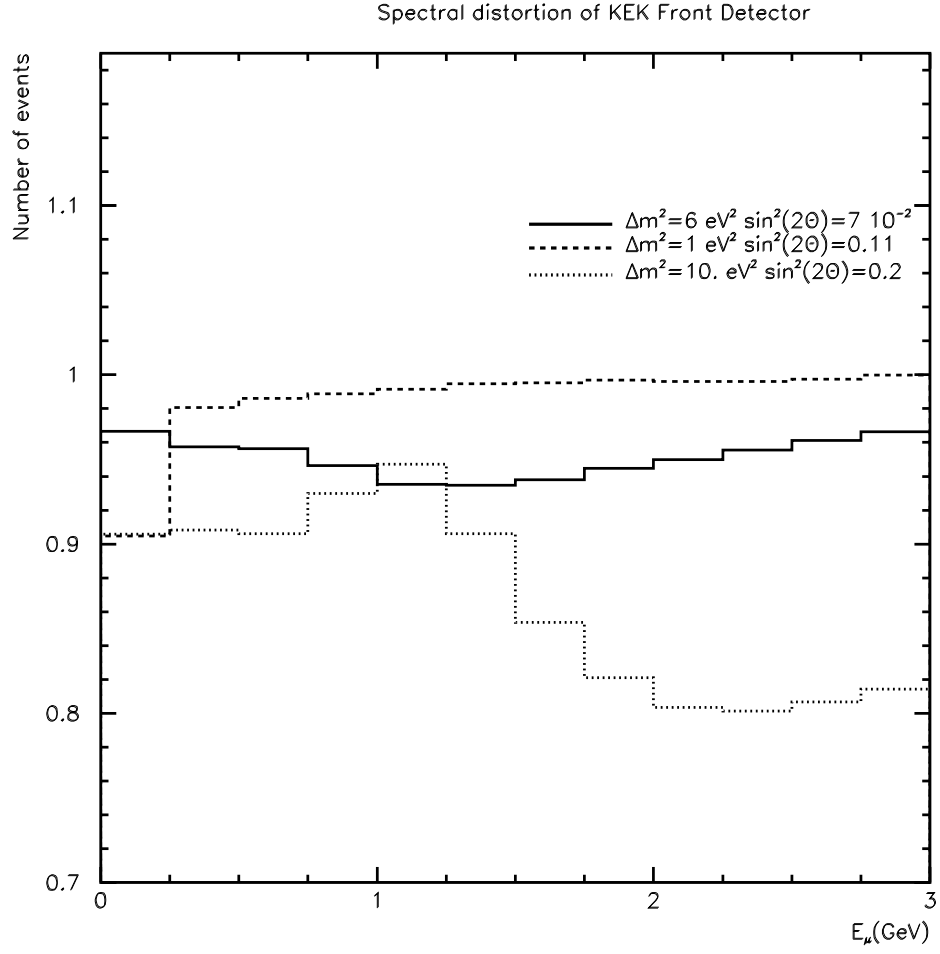
Figure 4: Distortion of the energy spectrum of the μ-like events due to oscillations in the KEK - front detector experiment. Shown are the ratios of the predicted numbers of events with and without oscillations for different values of the oscillation parameters.
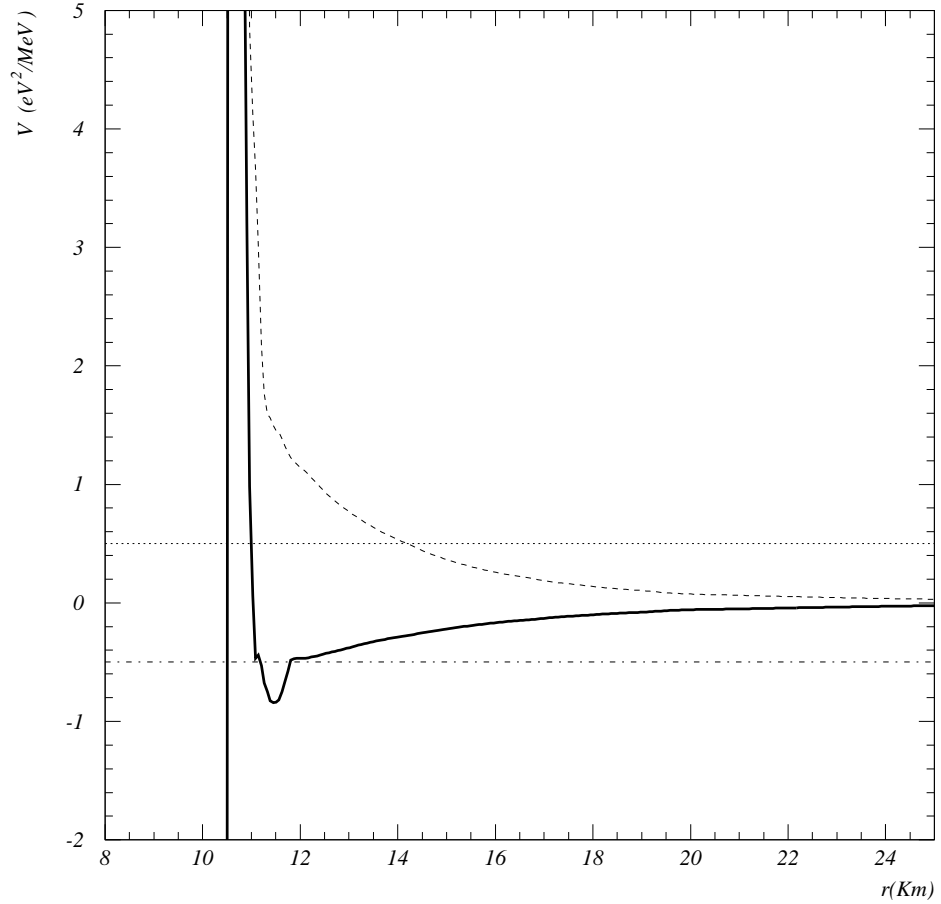
Figure 5: The matter potentials for the $\nu_e - \nu_s$ system in the supernova as the function of distance from the center of the star. Solid line shows the potential without neutrino background and the dashed line – with the background. The horizontal lines correspond to $\pm\Delta m^2_{LSND}/2E_\nu$ for $E_\nu = 10$ MeV and $\Delta m^2 = 10$ eV^2; the positive (negative) sign refers to neutrino (antineutrino) channel. Crossings of the potentials and the lines give the resonance points.
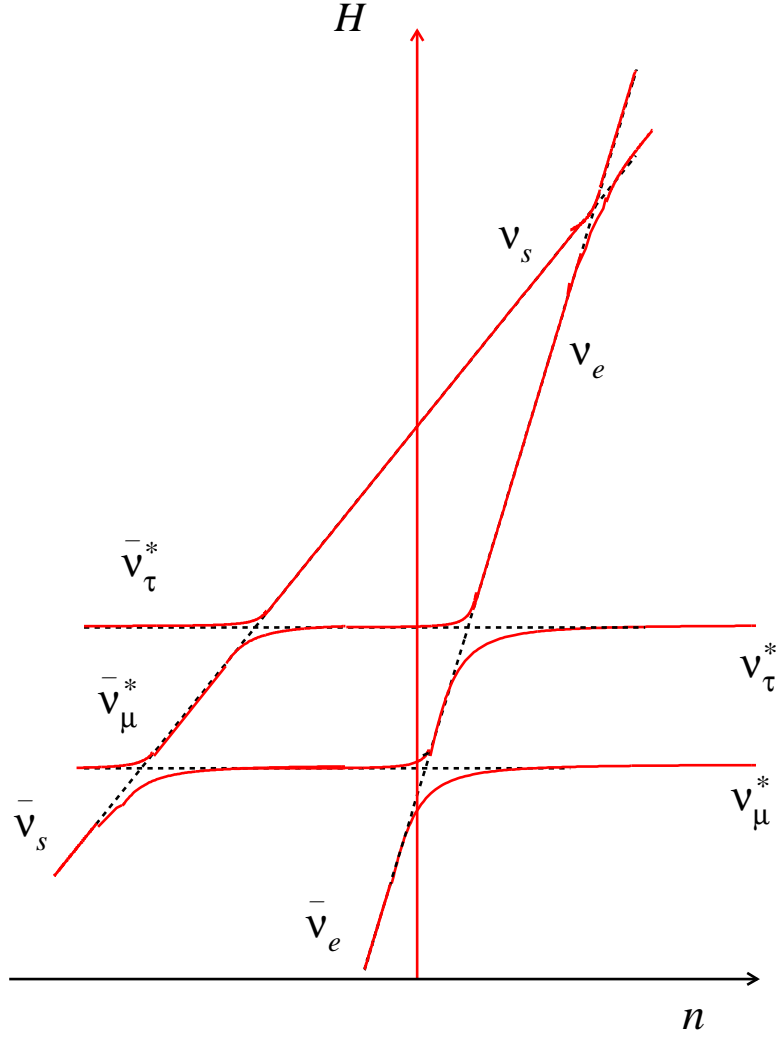
Figure 6: The level crossing diagram for the $(3 + 1)$ scheme with normal mass hierarchy in supernova. Solid lines show the dependence of the eigenstates of the effective Hamiltonian on the matter density. Dashed lines show the dependence of the flavor states. The semi-plane with $n > 0$ ($n < 0$) corresponds to the neutrino (antineutrino) channels. Only the outer resonance $\nu_e - \nu_s$ is shown.